Species-Specific Fish Feature Extraction Using Gabor Filters

Extracción Específica de la Especie Pescado Característica con Gabor Filtros

Extraction des Spécificités Propres á L'espèce de Poisson en Utilisant des Filtres Gabor

ARJUN KUMAR JOGINIPELLY[1]*, DIMITRIOS CHARALAMPIDIS[2], GEORGE IOUP[3],
JULIETTE IOUP[3] and CHARLES H. THOMPSON[4]

[1]*University of New Orleans, 6232 Waldo Drive, New Orleans, Louisiana 70122 USA. *arjunjoginipelly@gmail.com.*
[2]*University of New Orleans, Department of Electrical Engineering, New Orleans, Louisiana 70122 USA. dcharala@uno.edu.* [3]*University of New Orleans, Department of Physics, New Orleans, Louisiana 70148 USA. geioup@uno.edu. jioup@uno.edu.* [4]*NOAA Southeast Fisheries Science Center Stennis Space Center, Mississippi 39529 USA. charles.h.thompson@noaa.gov.*

ABSTRACT

Fish recognition and classification are challenging when performed on video data obtained in non-controlled environments (NCE's) such as in natural waters. Many NOAA Fisheries surveys use underwater cameras to gather video data for this purpose, which facilitate the analysis of fish populations. Since the amount of data is large, manual data analysis is insufficient. Automatic processing tools are necessary. Most techniques that extract features from fish are in two categories. In the first, features are specific to fish but not necessarily to a particular species. Yet, such measurements are often unreliable when extracted from video obtained in NCE's, since they strongly depend on the aspect of fish with respect to the camera. In the second, features are generic and may include texture and shape descriptors. Such features do not target specific species of interest. In this paper, we present an automatic technique using Gabor filters to extract characteristic features from two important species, namely, *Epinephelus morio* (which has a vertical band located at the tale) and *Ocyurus chrysurus* (which has a long horizontal line that runs across the body). The proposed algorithm is tested on 200 frames, each containing several fish and non-fish regions. The detection rate is 70.6% for *Epinephelus morio* and 80.3% for *Ocyurus chrysurus*, while 23.5% of the undetected *Epinephelus morio* cases do not have a visible tail band, and 16.7% of the undetected *Ocyurus chrysurus* cases do not have a visible straight body line. The false alarm rates are 3.8% and 2.1%, respectively.

KEY WORDS: Automated fish classification, automated fish feature extraction, image processing, Gabor filters, *Epinephelus morio*, *Ocyurus chrysurus*

BACKGROUND

Underwater video and still images are used by many programs within National Oceanic and Atmospheric Administration (NOAA) Fisheries with the objective of identifying and quantifying living marine resources. The NOAA Southeast Fisheries Science Center (SEFSC) – laboratories at Pascagoula, MS, Panama City, FL, and Beaufort, NC, all conduct annual fishery independent reef fish surveys using video, trap, and hook gear. The surveys target reef habitat and yield demographic data and abundance indices used in assessments for many federally managed species. Video techniques overcome the fish sampling limitations imposed by depth, fish behaviour, seafloor rugosity, and the selectivity inherent in hook, trap, and trawl methods (Cappo et al. 2006). In a given year, cameras are deployed at a large number of locations that are not amenable to sampling with nets or other means. Some of the systems use stereo pairs of cameras (Boynton and Voss 2005) that allow fish lengths to be estimated while others are used simply to identify and count the fish present. Analyses of the images from these surveys are used to produce indices of abundance and size distributions for the fish species observed. These data, in turn, are used in stock assessment models that ultimately influence regulations for the harvest of reef fish. Human analysts are required to view each image sequence to identify and enumerate fish species present at each location and measure their lengths. The process of manual analysis is both labour intensive and time consuming and is a significant limitation on how much this type of population sampling can be utilized. Automated image analysis capabilities are desperately needed in order to take full advantage of current image data collection technology.

Recent efforts to automate analysis of underwater images (Spampinato et al. 2010, Wilder 2010, Williams et al. 2012) of fish has focussed on detection and tracking of fish in sequences of images. Motion of the fish against a relatively static background has been exploited for detection and proven methods of object tracking (Li 2010) have been used to track fish from frame to frame. Accurate detection and tracking allows the number of fish present during a given time to be determined, but the ultimate goal is to count the number of fish of each species. Thus the next step in the process of automation is classification. A human analyst uses a multitude of cues to visually identify fish species. However, the primary features used are morphological properties such as shape of the body, head, fins, and tail and patterns in coloration. Two species having distinctive patterns in coloration that are frequently observed in survey images in the Gulf of Mexico are red grouper – *Epinephelus morio* (Valenciennes, 1828) and yellowtail snapper – *Ocyurus chrysurus* (Bloch, 1791) .

In underwater grayscale images, *Epinephelus morio* (EM) frequently display a light colored band near the margin of the caudal fin that contrasts strongly with a black band on the extreme margin. On the other hand, *Ocyurus chrysurus* (OC)

have, as their common name indicates, a yellow caudal fin. The same color extends in a tapering band along the side of the body through the eye to the anterior end of the head. In grayscale images, this band appears dark in contrast to the body's background color.

The two species were selected in this work for their great importance in the Gulf of Mexico. More specifically, EM is the most abundant grouper species in the Gulf of Mexico. It accounts for the bulk of the commercial grouper landings, and is the second most commonly caught grouper species recreationally. OC are fished along the US south Atlantic coast and south-eastern Gulf of Mexico. They are managed as a single stock with allowable catches distributed between the south Atlantic and Gulf of Mexico regions. Currently, the stock allowable biological catch (ABC) is set at 2.9 million pounds, with 0.725 million pounds (25% of ABC) going to the Gulf of Mexico.

Gabor Filters Used For Fish Feature Extraction

In this paper, Gabor filters (GF) are used to extract species-specific features from EM and OC. Gabor filters are widely used for texture segmentation (Fogel and Sagi 1989, Vyas and Regi 2006) and feature extraction (Shrivakshan 2011). In its most general form, the GF is a complex sinusoid (shown in Figure 1-A) modulated by a Gaussian (shown in Figure 1-B). An example of a GF filter is depicted in Figure 1-C. The mathematical representation of a horizontally oriented spatial GF is as follows:

$$h(x,y) = A\ exp\left\{-\frac{x^2}{2\sigma_x^2}-\frac{y^2}{2\sigma_y^2}\right\} exp\{2\pi i F x_r\} \quad (1)$$

where A is a constant, F is the spatial frequency, and σ_x and σ_y are the standard deviations of the GF in the x and y directions respectively. As will be described later in the paper, the feature extraction techniques employed in this work require that the filter is scaled according to the fish size. The GF filter was employed in this work owing to the ease with which its parameters can be tuned. The literature review of previous works on fish classification is found in Cadieux et al. (2000), Sampinato et al. (2010), Shrivakshan (2011), Wilder (2010), and Williams et al. (2012).

A GF oriented vertically exhibits a strong response for horizontal details as shown in Figure 2-A. Similarly, a GF oriented horizontally emphasizes vertical details as shown in Figure 2-B. The size of the filter is adjusted according to the size of the fish being tested by assigning the filter standard deviation to be proportional to the square root of the fish area. In other words,

$$\sigma_x^2 = \sigma_y^2 = \left(\alpha \times \sqrt[2]{Area}\right)$$

where α is a user defined constant empirically chosen to be 0.035.

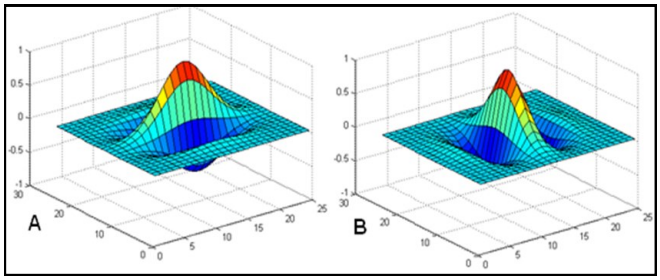

Figure 2. 2-D Gabor filters with $\sigma_x^2 = \sigma_y^2 = 4$
A. GF oriented vertically. B. GF oriented horizontally.

***Epinephelus morio* Feature Extraction Using Gabor Filters**

EM has a bright band on its tail, a feature that is specific to its species. An example is depicted in Figure 3-A. In order to detect this feature, the original fish image is first multiplied by its region mask, which is shown in Figure 3-B, to isolate the fish from its surroundings, as shown in Figure 3-C. The region mask is automatically obtained by subtracting the original image from the estimated background image (Piccardi 2004), and by setting equal to 1 (white) or 0 (black) all pixels that exceed or fall below user defined thresholds, respectively. The background image is obtained as the pixel-wise median of several frames (Han and Davis 2012). The resultant image is filtered separately with a horizontally and a vertically oriented GF to obtain images $I_{hor}(x,y)$ and $I_{ver}(x,y)$ as shown in Figures 4-A and 4-B, respectively. The image ratio,

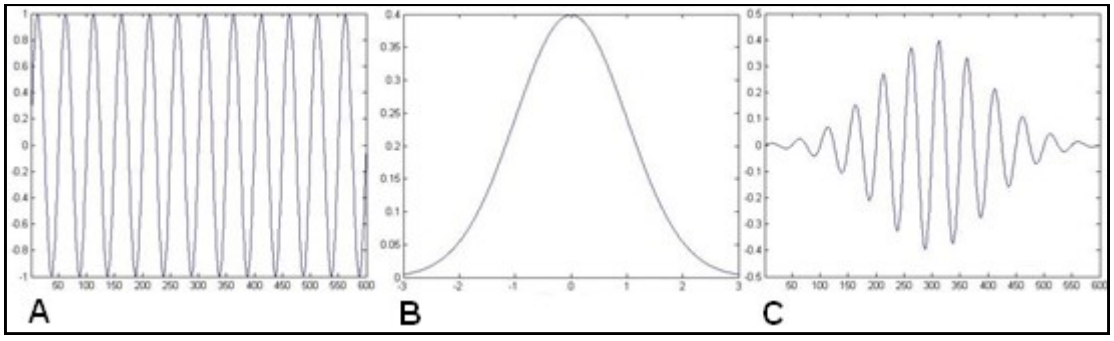

Figure 1. 1-D Gabor filter. A. Sinusoid. B. Gaussian. C. Gabor filter.

$$I_r(x,y) = I_{hor}(x,y) / I_{ver}(x,y)$$

is used to emphasize the stripe as shown in Figure 4-C. In order to eliminate the effect of vertical stripe-like edges in $I_{hor}(x,y)$ associated with the fish outline, a zone of pixels around the fish outline is set to zero. This is achieved by employing an erosion operation using a square structural element of size $[3 * \sigma_y] \times [3 * \sigma_y]$. In most cases, the edges are caused by the intensity difference between the fish region and the background.

In order to quantify the presence of the stripe, the following approach is used. First, a vertical moving average (MA) filter, $f_{MA}(y)$ of size $W_{EM} \times 1$ is applied on $I_r^{EM}(x,y)$ to emphasize cases of consecutive vertical high intensity pixels, such as vertical stripes. The value associated with W_{EM} is selected by calculating the square root of the area of the fish in each frame which is empirically chosen to be 21. The maximum value per column $m_{I_r}^{EM}(x)$ is computed for EM as follows:

$$m_{I_r}^{EM}(x) = \max_y \{f_{MA}(y) * I_r(x,y)\}$$

where * represents the convolution operation. The maximum value of $m_{I_r}^{EM}(x)$ namely,

$$m_{I_r}^{EM}(max) = \max_x \{m_{I_r}^{EM}(x)\}$$

quantifies the presence of a stripe in the fish region as shown in Figure 5. A median filter of size 3×1 is applied on $m_{I_r}^{EM}(x)$ to eliminate narrow spikes which are unlikely to correspond to the tail band.

Ocyurus chrysurus Feature Extraction Using Gabor Filters

The OC fish has a different feature specific to its species – a straight line across the fish body as depicted in Figure 6-A. A similar approach explained for EM is followed for OC to extract the horizontal line along the length of its body. An OC example is shown in Figure 6-A. Figure 6-B depicts the corresponding region mask, and Figure 6-C shows the isolated fish region. The resultant image is filtered separately with a vertically and a horizontally oriented GF to obtain images $I_{hor}(x,y)$ and $I_{ver}(x,y)$ as shown in Figures 7-A and 7-B, respectively. However, the ratio of the images in the OC case is computed as

$$I_r(x,y) = I_{ver}(x,y) / I_{hor}(x,y)$$

which highlights the horizontal line as shown in Figure 7-C. In order to eliminate the effect of horizontal stripe-like edges in $I_{ver}(x,y)$ associated with the fish outline, a zone of pixels around the fish outline is set to zero. This is achieved by employing an erosion operation using a square structural element of size. $[4.8 * \sigma_y] \times [4.5 * \sigma_y]$

It can be observed in Figure 7-A that the straight line is darker than the rest of the OC body. On the other hand, detecting the EM tail band is a maximization problem. For consistency with the EM technique, detecting the OC straight body line is converted to a maximization problem by subtracting the value of each pixel in the ratio image $I_r(x,y)$ from the maximum intensity of $I_r(x,y)$.

A horizontal MA filter of size $1 \times W_{OC}$ is applied along the rows of $I_r(x,y)$. (The OC straight line runs across the fish body and thus strongly depends on the fish size. For

Figure 3. EM pre-processing steps. A. Original image of EM with indicator for vertical stripe at the end of tale. B. Region mask of EM. C. Pre-processed image of EM.

Figure 4. Filtering results of horizontal and vertical Gabor filters on EM.
A. Filtering result of horizontal Gabor filter. B. Filtering result of vertical Gabor filter. C. Ratio image.

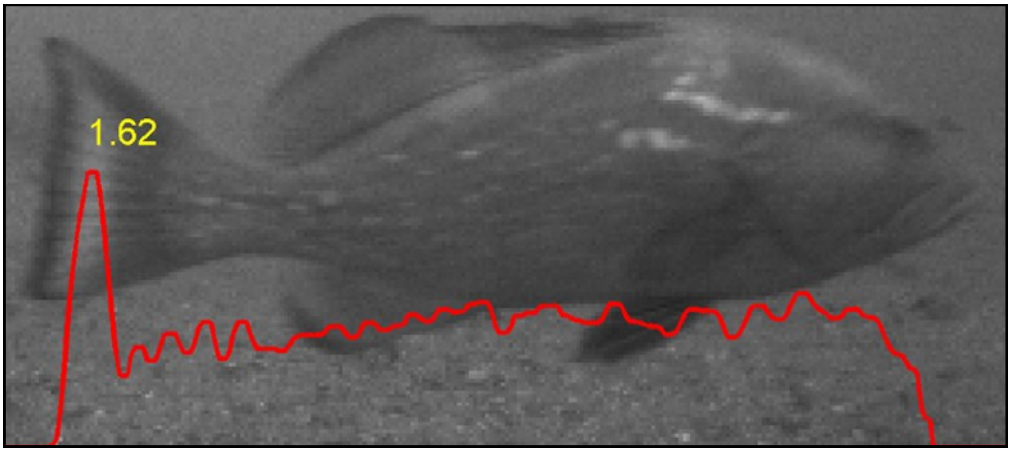

Figure 5. EM tail band detection – maximum value per column $m_{I_r}^{EM}(x)$

Figure 6. OC pre-processing steps. A. Original image of OC with indicator for horizontal line. B. Region mask of OC. C. Pre-processed image of OC.

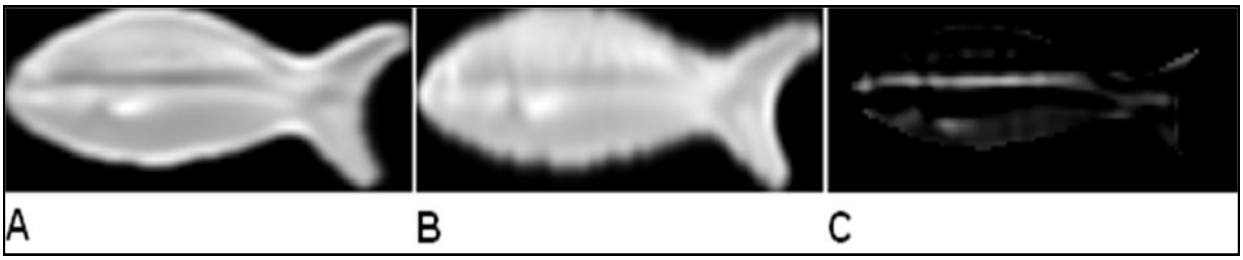

Figure 7. Filtering results of horizontal and vertical Gabor filters on OC. A. Filtering result of horizontal Gabor filter. B. Filtering result of vertical Gabor filter. C. Ratio image. $I_r(x,y)$

this reason, the value associated with W_{OC} is selected automatically, and is set to be proportional to the square root of the fish area. The maximum value for each row is computed as:

$$m_{I_r}^{OC}(y) = max_x\{f_{MA}(x) * I_r(x,y)\} \quad (3)$$

where * represents the convolution operation.
The maximum value of, $m_{I_r}^{OC}(y)$ namely,

$$m_{I_r}^{OC}(max) = \max_x\{m_{I_r}^{OC}(y)\}$$

quantifies the presence of the straight line in the fish region as shown in Figure 8.

When a fish is oriented at an angle with respect to *x*-axis as shown in Figure 9-E, the straight line may not be exactly horizontal and may not be detected by the algorithm. For this reason, the original fish image, $OF_r(x,y)$, as shown in Figure 9-E, is rotated by different angles, and the largest is $m_{I_{rmax}}^{OC}$ considered.

From Figure 9 it is evident that the plot corresponding to the maximum $m_{I_{rmax}}^{OC}$ is the one for which the OC line is horizontal.

In this particular example, the image is rotated in steps of 10^0 from -40^0 to 40^0 and the largest $m_{I_{rmax}}^{OC}$ is obtained when the image is rotated at 10^0 as shown in Figure 9-F. The fish orientation is not a significant issue for

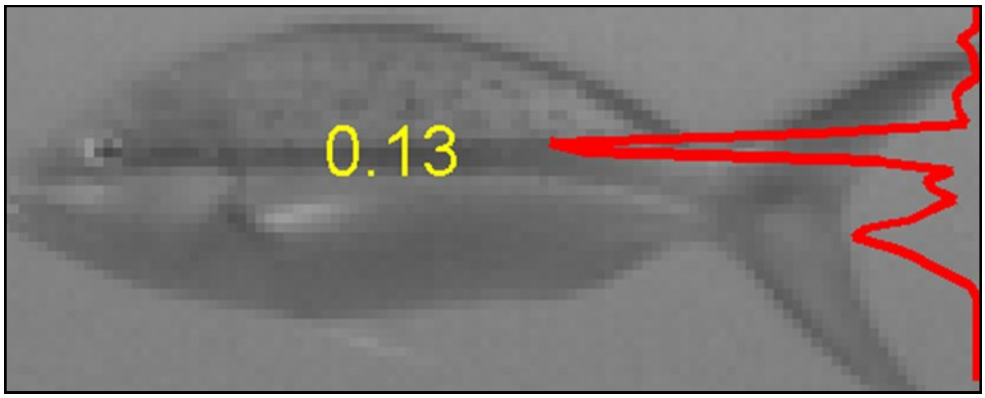

Figure 8. OC straight line detection – maximum value per row $m_{I_r}^{OC}(y)$

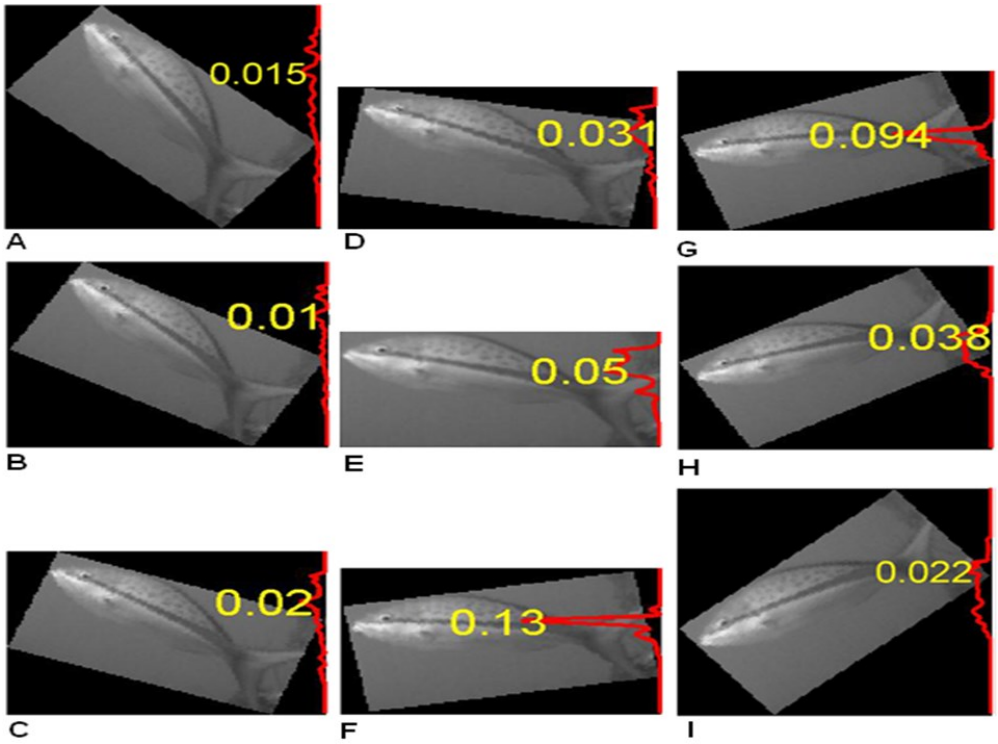

Figure 9. OC straight line detection when the fish is oriented at a different angle with respect to *x* axis. A. -40°. B. -30°. C. -20°. D. -10°. E. 0° (which is also the original view of the OC fish). F. 10°. G. 20°. H. 30°. I. 40°.

EM, since the tail band is relatively short and wide, as opposed to the OC straight line which is relative long and narrow.

The algorithm for detection and classification of OC fish species is shown in Figure 10. The algorithm described earlier for the classification of EM species is similar to the algorithm presented in Figure 10 if the iterative process involving the rotation of image and region mask is removed.

RESULTS AND DISCUSSION

In this section, the performance of the algorithm is discussed in terms of detection and false alarm rates. The algorithm was tested on sequence of 200 images from an annual reef fish survey conducted by the SEFSC Pascagoula laboratory. The total number of EM, OC, and non-EM/non-OC fishes are provided in Table 1.

The results for EM are summarized in Table 2. An EM fish is detected when the $m_{I_r}^{EM}(max)$ value is found to be between two thresholds.

More specifically, $T_1^{EM} < m_{I_r}^{EM}(max) < T_2^{EM}$

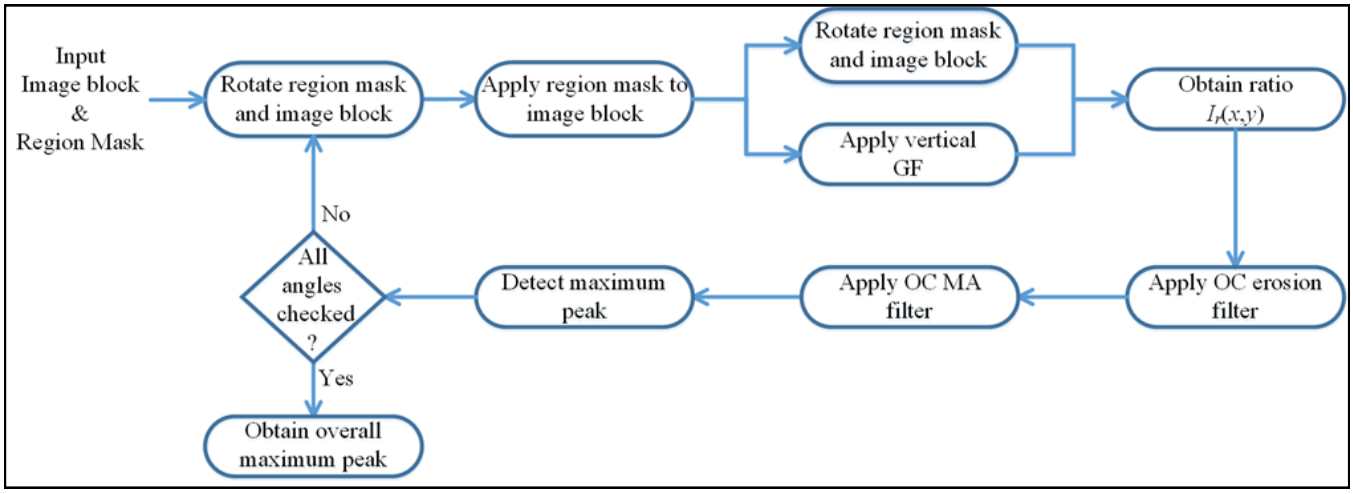

Figure 10. Proposed algorithm flowchart. The OC detection algorithm. The EM detection algorithm is similar if the process involving the rotation of the image and region mask is eliminated.

The threshold values were empirically chosen as $T_1^{EM} = 0.95$ and $T_2^{EM} = 2$

Any region with corresponding $m_{I_r}^{EM}(max)$ peak outside the range specified by the two thresholds is categorized as non-EM. Such a region may correspond to a non-EM fish or to a non-fish object. The purpose of the lower threshold, T_1^{EM} is to separate regions which contain a significant vertical band from regions that do not include such a band. It was observed that in some cases non-fish regions included some apparent vertical stripes, which however result in exceptionally $m_{I_r}^{EM}(max)$ high peaks. The higher threshold, T_2^{EM} is used to identify such non-fish regions.

As can be observed from Table 2, the total number of EM not detected by the proposed algorithm is 20, which corresponds to 29.4% of the EM cases. However, in the vast majority of missed cases (16 or 23.5%) the video frame itself has no or little information about the tail band. Two examples of such missed cases are shown in Figure 11. Figure 11-A depicts a case where the tail is positioned in a way that the band is only slightly visible, and Figure 11-D shows an example where the fish is facing the camera. Function $m_{I_r}^{EM}(x)$ is depicted as a red curve, and the value shown indicates the maximum peak, $m_{I_r}^{EM}(max)$. Even human analysts, who may be capable of recognizing the fish as EM, may not be able to distinguish the tail band in these two examples.

On the other hand, the algorithm is capable of detecting EM even when fishes merge together. An example is illustrated in Figure 11-C, where it is clearly shown that the $m_{I_r}^{EM}(max)$ peak is found at the tail band.

Figure 11-B shows a non-EM fish example, which is correctly detected as non-EM, since the fish does not have a tail stripe. According to the results presented in Table 2, the vast majority of the non-EM cases are correctly detected as non-EM. Only 3.8% of the non-EM cases are categorized as EM. In particular, 2.1% and 1.7% of the false alarm cases correspond to other fish and non-fish regions, respectively.

The results for OC are summarized in Table 3. Similar to the EM case, an OC fish is detected when the $m_{I_r}^{OC}(max)$ value is found to be between two thresholds. In other words, $T_1^{OC} < m_{I_r}^{OC}(max) < T_2^{OC}$. The threshold values were empirically chosen as $T_1^{OC} = 0.06$ and $T_2^{OC} = 0.2$

Any region with corresponding $m_{I_r}^{OC}(max)$ peak outside the range specified by the two thresholds is categorized as non-OC. Regions with associated $m_{I_r}^{OC}(max)$ peak below the lower threshold, T_1^{OC} do not include a significant

horizontal line. The higher threshold, T_2^{OC} is used for the same reason as in the case of EM.

As can be observed from Table 3, the total number of OC not detected by the proposed algorithm is 13, which corresponds to 19.7% of the OC cases. As in the case of EM, for the majority of missed cases (11 or 16.7%) the video frame itself has no or little information about the straight line. Two examples where the straight line is not clearly visible are presented in Figures 11-E and Figure 11-G. Figure 11-F shows a non-OC fish example, which is correctly detected as non-OC, since the fish does not have a horizontal line.

Table 1. Information about reef fish images obtained from SEFSC Pascagoula laboratory

Total number of frames used for experimentation	200
Total number of EM available in total frames	68
Total number of OC available in total frames	66
Total number of non-EM and non-OC fish available in total frames	159
Total number of non-fish objects available in total frames	74

Table 2. EM results

EM	Correctly detected		48 (70.6%)
	Not Detected	Technique not successful (missed detection)	4 (5.9%)
		Due to non-visible tail band	16 (23.5%)
Non-EM	Other fish detected as EM (false alarm)		5 (2.1%)
	Other fish correctly not detected as EM		154 (66.1%)
	Non-fish objects detected as EM (false alarm)		4 (1.7%)
	Non-fish objects correctly not detected as EM		70 (30.0%)

Table 3. OC results

OC	Correctly detected		53 (80.3%)
	Not detected	Technique not successful (missed detection)	2 (3.0%)
		Due to non-visible horizontal line	11 (16.7%)
Non-OC	Other fish detected as OC (false alarm)		4 (1.7%)
	Other fish correctly not detected as OC		155 (66.5%)
	Non-fish objects detected as OC (false alarm)		1 (0.4%)
	Non-fish objects correctly not detected as OC		73 (31.3%)

Function $m_{I_r}^{OC}(y)$ is depicted as a red curve, and the value shown indicates the maximum peak, $m_{I_r}^{OC}(max)$.

The proposed algorithm detected a total of 5 false alarms (i.e., non-OC regions detected as OC), which is only 2.1% of the non-OC cases. In particular, 1.7% and 0.4% of the false alarm cases correspond to other fish and non-fish regions, respectively. Figure 12 illustrates a few examples where non-EM/non-OC species are detected as EM or OC. Figure 13 presents a few examples where non-fish objects are detected as EM or OC. Some examples where the proposed algorithm missed detection of EM and OC are shown in Figure 14.

CONCLUSIONS

The authors presented a technique based on GFs to effectively extract species-specific features from *EM* and *OC fish species*. These features are used for detecting EM and OC fish species. The detection rate is 70.6% for EM and 80.3% for *OC*, while 23.5% of the undetected *EM* cases do not have a visible tail band, and 16.7% of the undetected *OC* cases do not have a visible straight body line. Therefore, missed detection for these cases is expected. The false alarm rates are only 3.8% and 2.1%, respectively. These results are promising and indicate that these features may complement other feature extraction techniques for the purpose of fish classification. Additionally, target tracking may be used to associate the same fish region in different frames, so that the whole fish sequence is classified as a single species, even if detection is successful in only one of the frames. Even if false alarms occur, automatic detection significantly reduces the amount of data to be examined by human analysts.

LIST OF ABBREVIATIONS USED

SEFSC – Southeast Fisheries Science Center
NOAA – National Oceanic and Atmospheric Administration.
EM – *Epinephelus morio* or red grouper
OC – *Ocyurus chrysurus* or yellow tail snapper
ABC – Allowable Biological Catch
GF – Gabor Filters
MA – Moving Average

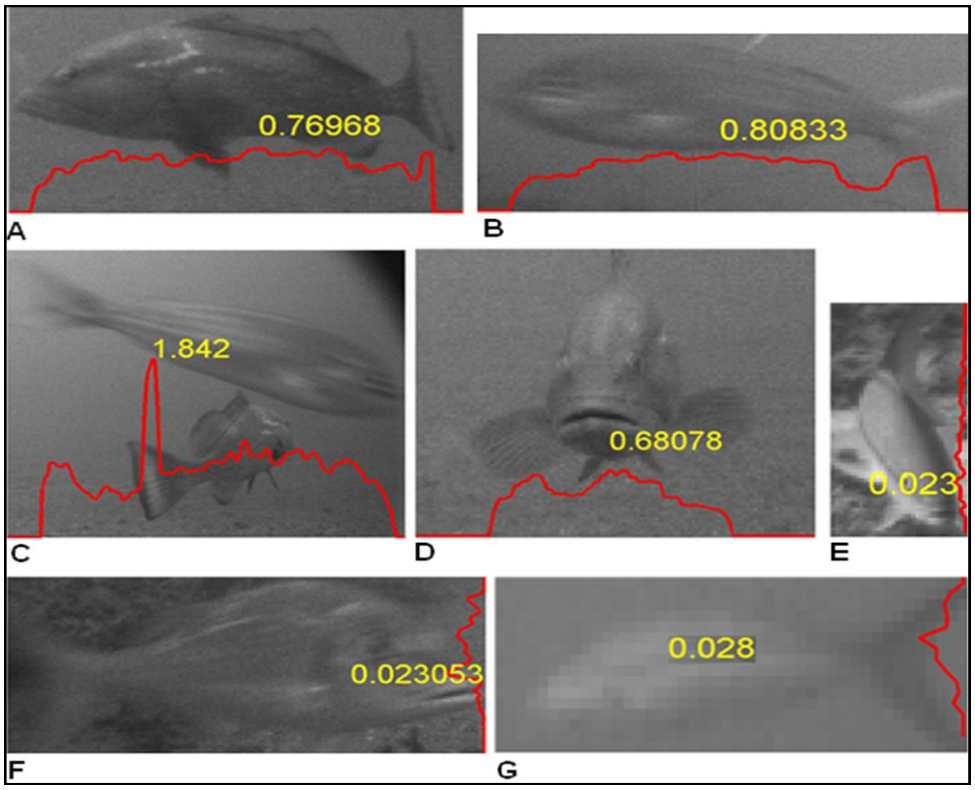

Figure 11. Illustration of some EM and OC results
A. EM tail is positioned in a way that the tail band is only slightly visible. B. As expected, the EM fish is detected as non-EM since the tail band is not visible. C. EM tail band is detected even though the two fishes merged. D. As anticipated, the EM fish is detected as non-EM since the fish is facing the camera and the tail band is not visible. E. The OC fish is not detected since the straight line is not clearly visible. F. As anticipated, the OC fish is detected as non-OC since the fish does not appear to have a straight line. G. As expected, the OC fish is not detected since the straight line is not visible, mainly due to the low image resolution.

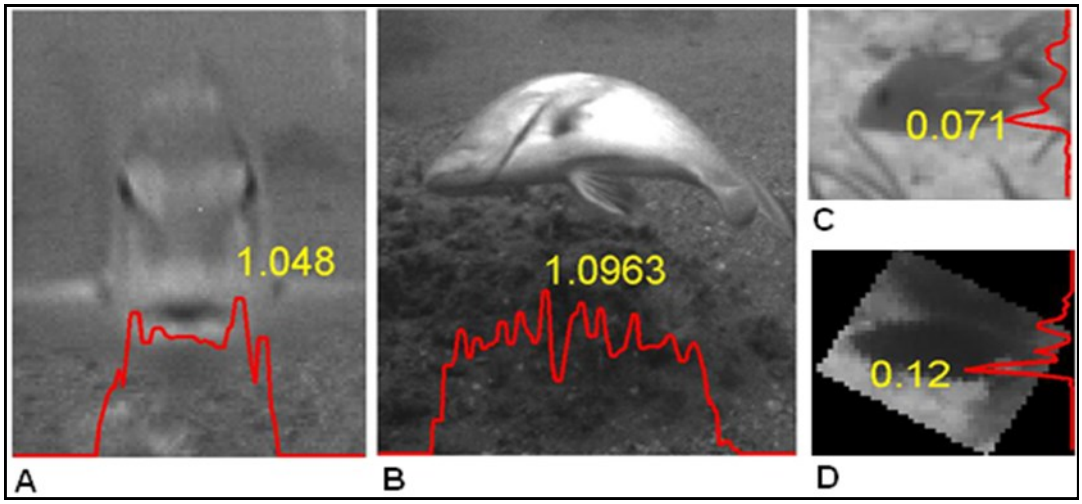

Figure 12. Illustration of few cases of false alarms (non-EM detected as EM, or non-OC detected as OC). — A. Fish detected as EM although there is no visible tail band information. B. Fish detected as EM although there is no visible tail band. C. Fish detected as OC although there is no clear visibility of straight body line. D. Fish detected as OC although there is no clear visibility of straight body line.

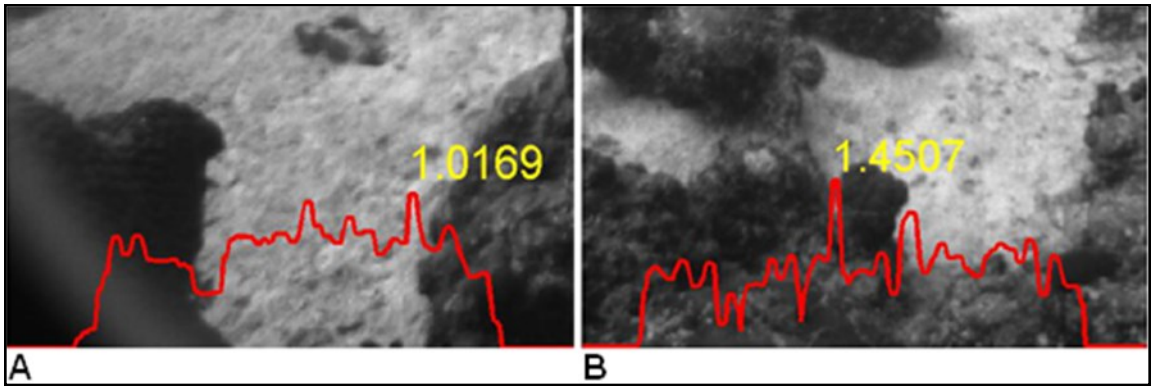

Figure 13. Illustration of few cases of false alarms (non-fish detected as EM or OC)
A. The algorithm detected non-fish as EM. B. The algorithm detected non-fish as EM.

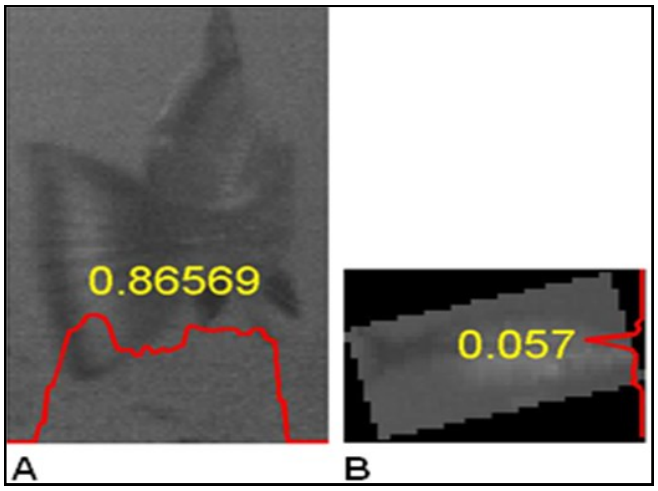

Figure 14. Illustration of few cases where EM and OC are not detected by the algorithm.
The technique is unsuccessful in detecting EM although the tail band is clearly visible. B. The technique failed in detecting OC although the straight line is clearly visible.

ACKNOWLEDGEMENTS

This work was supported by a grant from NOAA Fisheries Advanced Sampling Technology Working Group. The project was NASA (2011)-STENNIS-02 "Feature Analysis for Classification of Fish in Underwater Video" with University of New Orleans award number CON000000001307.

LITERATURE CITED

Boynton, C.G. and K.J. Voss. 2005. An Underwater Digital Stereo Video Camera for Fish Population Assessment. *A Final Report for NOAA Fisheries Coral Reef Program*.

Cadieux, S, F. Michaud, and F. Lalonde. 2000. Intelligent System for Automated Fish Sorting and Counting. *IEEE International Conference on Intelligent Robots and Systems* **2**:1279-1284.

Cappo, M., E. Harvey, and M. Shortis. 2006. Counting and measuring fish with baited video techniques – an overview. *Workshop Proceedings Australian Society* **2006**:101-114.

Fogel, I. and D. Sagi. 1989. Gabor Filters as Texture Discriminator. *Biological Cybernetics Journal* **61**:103-113.

Han, B. and L.S. Davis. 2012 Density-Based Multi-Feature Background Subtraction with Support Vector Machine. *IEEE Transactions on Pattern Analysis and Machine Intelligence* **34**:1017-1023.

Li, X. 2010. A Multiple Object Tracking Method using Kalman Filter. *IEEE Conference on Information and Automation* **June 2010**:1862-1866.

Piccardi, M. 2004. Background Subtraction Techniques: A Review. *IEEE International Conference on Systems, Man and cybernetics* **4**:3099-3104.

Shrivakshan, G.T. 2011. Detecting the age of fish through image processing using its morphological features. *International Journal of Computer Science and Information Technologies* **2**:2562-2567

Spampinato, D.C. and R.B. Fisher. 2010. Automatic Fish Classification for Underwater Species Behaviour Understanding. *ACM International Workshop on Analysis and Retrieval of Tracked Events and Motion in Imagery Streams* **October 2010**:45-50.

Vyas, V.S. and P. Rege. 2006. Automated Texture Analysis with Gabor Filters. *International Journal on Graphics, Vision and Image Processing* **July 2006**: 6.

Wilder, J.D. 2010. System Integration and Image Pre-Processing for an Automated Real-Time Identification and Monitoring System for Coral Reef Fish. MS.Thesis The State University of New Jersey, New Brunswick, New Jersey USA.

Williams, K., C. Rooper, and J. Harms. 2012. Report of the National Marine Fisheries Service Automated Image Processing Workshop. NOAA Technical Memorandum NMFS-F/SPO-121.